Theoretical Formulation of Nonadiabatic Electrochemical Proton−Coupled Electron Transfer at Metal−Solution Interfaces

ARTICLE *in* THE JOURNAL OF PHYSICAL CHEMISTRY C · JULY 2008

Impact Factor: 4.77 · DOI: 10.1021/jp802171y

3 AUTHORS, INCLUDING:

Alexander V. Soudackov
University of Illinois, Urbana-Champaign
54 PUBLICATIONS **1,753** CITATIONS

Theoretical Formulation of Nonadiabatic Electrochemical Proton-Coupled Electron Transfer at Metal−Solution Interfaces

Charulatha Venkataraman, Alexander V. Soudackov, and Sharon Hammes-Schiffer*

Department of Chemistry, 104 Chemistry Building, Pennsylvania State University, University Park, Pennsylvania 16802

Received: March 12, 2008; Revised Manuscript Received: April 15, 2008

Expressions are derived for the nonadiabatic transition probabilities, the heterogeneous rate constants, and the current densities of electrochemical proton-coupled electron transfer (PCET) reactions. In these reactions, an electron is transferred between a solute complex and a metal electrode concurrently with proton transfer within the hydrogen-bonded solute complex. The reaction is described in terms of nonadiabatic transitions between reactant and product electron−proton vibronic states. The current densities are obtained by explicit integration over the distance between the solute complex and the electrode, thereby accounting for the effects of extended electron transfer. These systematic derivations are based on a series of well-defined approximations, leading to a series of analytical expressions for the heterogeneous rate constants and current densities that are valid in specified regimes. The resulting expressions are compared with the analogous expressions for electrochemical electron transfer (ET), and specific characteristics of the current densities that implicate PCET are identified. The strong dependence of the vibronic coupling on the proton donor−acceptor distance for PCET leads to additional terms in the electrochemical PCET rate constant expressions. The total reorganization energy includes two additional contributions: the reorganization energy of the proton donor−acceptor mode and a coupling term associated with the modulation of the vibronic coupling by this mode. The rate constants also include an additional exponential temperature-dependent prefactor that depends on the frequency of this mode and a parameter characterizing the modulation of the vibronic coupling by this mode. This prefactor leads to non-Arrhenius behavior of the rate constants at higher temperatures. Furthermore, the effective activation energies contain temperature-dependent terms arising from the change in the equilibrium proton donor−acceptor distance upon electron transfer. This term has a different sign for the cathodic and anodic processes, leading to asymmetries of the Tafel plots, even for small changes in the equilibrium distance. These characteristics of electrochemical PCET are illustrated by calculations for model systems. This theoretical formulation is applicable to a wide range of experimentally studied electrochemical PCET reactions.

1. Introduction

The coupled transfer of electrons and protons is essential for a broad range of chemical and biological processes. The mechanisms of these processes involve a complex interplay of consecutive electron transfer (ET) and proton transfer (PT) steps and concurrent steps in which the electron and proton are transferred simultaneously without a well-defined intermediate. The latter mechanism is often favorable because it avoids high-energy intermediates, although other factors, such as reorganization energy and coupling, must also be taken into account. The concurrent transfer of an electron and a proton has been denoted proton-coupled electron transfer (PCET).

Electrochemical methods are highly suitable for probing the detailed mechanisms of PCET reactions because the reaction can be controlled easily through the electrode potential, and observables such as current density can be measured with high precision. For example, Finklea and co-workers have attached redox couples to self-assembled monolayers on electrodes and have measured the rates for one-electron, one-proton redox chemistry over a wide range of overpotentials for both the oxidation and the reduction steps.[1−4] The dependence of the rates on pH and the kinetic isotope effects for an osmium aquo complex attached to a mixed self-assembled monolayer on a gold electrode support a PCET mechanism.[3,4] The PCET mechanism has also been suggested for the reduction of water−superoxide ion complexes,[5] the redox chemistry of substituted benzoquinones with carboxylates as proton acceptors,[6] and the oxidation of hydrogen-bonded phenols.[7,8]

The theoretical aspects of electrochemical ET have been developed extensively over the past several decades,[9−28] in some cases including bond breaking and hydrogen discharge processes.[12,13,29−33] In comparison, electrochemical PCET has attracted the attention of theoreticians only relatively recently.[5,34−36] On the other hand, the theory of homogeneous PCET reactions has been well-developed over the past decade.[38−42] Recently, Costentin, Savéant, and co-workers[35,43] have modified portions of the homogeneous nonadiabatic PCET theory[38−42] to reflect the electrochemical environment in certain limits. Schmickler and co-workers[34,36] have presented an alternative approach based on the Anderson−Newns model Hamiltonian[44,45] that has been used widely in the theory of electrochemical ET. In principle, this alternative approach can be generalized to describe the dynamics of both nonadiabatic and adiabatic electrochemical PCET reactions. We are also exploring this direction in a separate manuscript.[46]

In the present paper, we extend our theory for homogeneous PCET[40−42] to electrochemical PCET using the methods and techniques developed for electrochemical ET. Our objective is

* Corresponding author. E-mail: shs@chem.psu.edu.

10.1021/jp802171y CCC: $40.75
Published on Web 07/23/2008

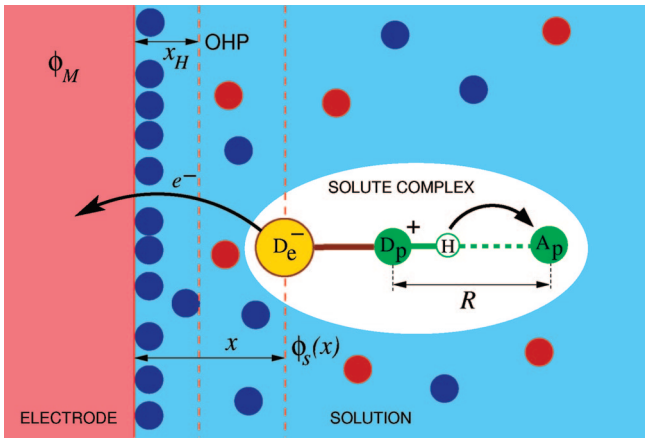

Figure 1. Schematic picture of the electrochemical PCET reaction system consisting of a solute complex near the surface of a metal electrode in solution. The electron transfers from the electron donor D_e of the solute complex to the electrode, and the proton transfers from D_p to A_p within the solute complex. Filled circles represent the ions of the supporting electrolyte in the solvent. ϕ_M is the inner potential of the electrode, and $\phi_s(x)$ is the electrostatic potential in solution at a distance x from the electrode surface. x_H is the distance to the outer Helmholtz plane (OHP), which is assumed to be the plane of closest approach for the solute complex. R is the proton donor−acceptor distance within the solute complex.

to present a systematic derivation of expressions for heterogeneous rate constants and current densities for nonadiabatic electrochemical PCET based on a series of well-defined approximations. This procedure leads to a series of expressions that are valid in specified regimes. We also compare the resulting expressions to the analogous expressions for electrochemical ET and identify experimentally measurable characteristics of the current densities that would implicate PCET reactions.

An outline of the paper is as follows. In section 2, we define the reaction system for electrochemical PCET, describe the general theoretical formulation, and derive the expressions for the heterogeneous rate constants and current densities. In section 3, we apply this approach to simple model systems to illustrate the characteristics that are specific to electrochemical PCET reactions. Section 4 presents a summary of the various expressions provided in section 2, compares these expressions to the electrochemical ET counterparts, and provides an outlook for future directions.

2. Theory

A. Electrochemical PCET Reaction System. The electrochemical PCET system consists of a metal electrode immersed in a solution containing solute molecules capable of exchanging electron(s) with the electrode concurrently with a proton transfer reaction. We assume that the proton transfer occurs within a hydrogen-bonded solute complex and that the electron transfer reaction does not occur unless the hydrogen-bonded solute complex is formed. The solute complex could be either a single solute molecule with an internal hydrogen bond or a solute molecule hydrogen-bonded to another molecule, such as a buffer or solvent. Figure 1 depicts this type of general electrochemical PCET system. As depicted in this figure, the solute complex consists of an electron donor group, D_e; a proton donor group, D_p; a proton acceptor group, A_p; and a transferring proton, H.

The reversible electron transfer process between the solute complex (SC) and the metal electrode (M) can be represented as

$$SC + M \rightleftharpoons SC^+ + M[e^-(\epsilon_m)] \quad (1)$$

where $e^-(\epsilon_m)$ indicates that the transferred electron occupies the metal one-electron level with energy ϵ_m. As in models for electrochemical ET,[47] we consider the case when the electron transfer reaction between the solute complex and the electrode can occur at any distance $x \geq x_H$ from the electrode surface, where x_H is the distance corresponding to the outer Helmholtz plane. Due to the formation of the electrical double layer, the electrostatic potential in the solution at a distance x from the electrode is $\phi_s(x)$, where the potential for the bulk solvent is defined to be zero (i.e., $\phi_s(\infty) = 0$). We assume that the potential $\phi_s(x)$ arises solely from the supporting electrolyte ions with charges $\pm z_{el}$ and that the contribution of the solute complex (i.e., the redox ions) to the potential $\phi_s(x)$ is negligible. This assumption is typically reasonable because the concentration of the redox ions is usually significantly smaller than the concentration of the supporting electrolyte ions.[47] The inner potential of the electrode is ϕ_M, and the metal one-electron energy levels, ϵ_m, are defined relative to the chemical potential (Fermi energy), μ_M, of the electrode for $\phi_M = 0$.

Nuclear and Electronic Subsystems. This general electrochemical PCET system is composed of both nuclear and electronic subsystems. The nuclear subsystem includes the following degrees of freedom: the transferring hydrogen coordinate, r_p; the distance R between the proton donor and acceptor within the solute complex; and the solvent translational and orientational degrees of freedom, ξ. Note that the proton coordinate, r_p, can be three-dimensional. The proton donor−acceptor vibrational mode, R, has been shown to play a crucial role in the description of proton transfer[48−53] and PCET reactions.[42] The remaining intramolecular degrees of freedom of the solute complex dynamically uncoupled from the electron and proton transfer reactions can also be included in the formulation using the conventional methodology developed for ET reactions.[41,54,55] For simplicity, however, we neglect these effects in the present paper.

The electronic subsystem includes all electrons of the solute complex, the electrons in the metal electrode, and the electrons localized on the solvent molecules. For simplicity, we adopt the Born−Oppenheimer approximation for the solvent electrons, assuming that they are infinitely fast on the time scale of the electron and proton transfer reactions and, thus, adjust instantaneously to the charge distribution in the solute complex.[56] Their "solvating" effect can be included in the solute−solvent interaction potential. For the electrons in the conduction band of the metal electrode, we use the effective one-electron model, in which the electrons in the metal occupy highly delocalized one-electron states with probabilities defined by the Fermi distribution function,

$$f(\epsilon_m) = [1 + e^{\beta\epsilon_m}]^{-1} \quad (2)$$

where $\beta = 1/k_B T$.

The electronic states of the solute complex can be described in terms of four valence bond states,[37] analogous to the case of homogeneous PCET.[40] The electronic wave function, $|\Psi_I\rangle$, of the reduced solute complex SC is represented as a linear combination of the two valence bond states, $|\psi_{1a}\rangle$ and $|\psi_{1b}\rangle$, corresponding to the reactant and product electronic basis states for the proton transfer reaction:

$$\begin{aligned} &(1a) \quad D_e^{\ominus}-D_p^{\oplus}-H\cdots A_p \\ &(1b) \quad D_e^{\ominus}-D_p\cdots H-A_p^{\oplus} \end{aligned} \quad (3)$$

where the indices a and b denote the states with the proton

bonded to the proton donor and proton acceptor, respectively. Here, we assume that $|\Psi_I\rangle$ corresponds to the electronically adiabatic ground state in this basis with energy $\mathcal{E}_I^0(r_p, R, \xi)$. The superscript "0" on the energy denotes that the solute complex is in bulk solution, where $\phi_s = 0$. Analogously, the electronic wave function $|\Psi_{II}\rangle$ of the oxidized solute complex SC^+ is represented as a linear combination of the two valence bond states $|\psi_{2a}\rangle$ and $|\psi_{2b}\rangle$:

$$\begin{array}{ll}(2a) & D_e-D_p^{\oplus}-H\cdots A_p \\ (2b) & D_e-D_p\cdots H-A_p^{\oplus}\end{array} \tag{4}$$

Analogous to the reduced state of the solute complex, $|\Psi_{II}\rangle$ corresponds to the electronically adiabatic ground state in this basis with energy $\mathcal{E}_{II}^0(r_p, R, \xi)$. Here, the electron has been transferred to the metal electrode.

Hamiltonian of the Reaction System. The total Hamiltonian, $\hat{H}_{tot}$, of the electrochemical PCET system can be expressed as a sum of the unperturbed Hamiltonian, $\hat{H}_0$, which describes the solvated solute complex and the electrode, and the perturbation, $\hat{V}$, which describes the coupling between the solute complex and the electrode corresponding to electron exchange. The unperturbed Hamiltonian can be expressed as

$$\hat{H}_0 = \hat{T}_p + \hat{T}_R + \hat{T}_\xi + \hat{H}_{el} \tag{5}$$

where $\hat{T}_p$, $\hat{T}_R$, and $\hat{T}_\xi$ are the kinetic energy operators for the proton, R mode, and solvent modes, respectively. The electronic Hamiltonian is composed of two terms:

$$\hat{H}_{el} = \hat{H}_M + \hat{H}_s(\mathbf{r}_e, r_p, R, \xi) \tag{6}$$

where $\mathbf{r}_e$ denotes the electron coordinates, $\hat{H}_M$ is the effective one-electron Hamiltonian of the electrons in the conduction band of the metal electrode, and $\hat{H}_s$ is the Hamiltonian of the solvated solute complex. $\hat{H}_s$ includes the gas-phase solute Hamiltonian, the interaction of the solute complex with the solvent molecules, the interaction of the solute complex with the electrostatic potential $\phi_s(x)$, and the solvent−solvent interactions.

Next, we define the initial and final diabatic electronic states of the entire system for the forward reaction with respect to the electronic Hamiltonian $\hat{H}_{el}$. The initial electronic state, $|\Psi_i\rangle$, corresponds to the solvated solute complex in its reduced form SC. As defined previously, the reduced solvated solute complex has energy $\mathcal{E}_I^0(r_p, R, \xi)$ in bulk solution where $\phi_s = 0$. Extra work is required to move the solute complex with total charge ze from the bulk solution at zero potential to a point at a distance x from the electrode surface with potential $\phi_s(x)$.[9,57] Note that the potential $\phi_s(x)$ is defined to be the potential due to the electrical double layer from the supporting electrolyte ions in the absence of the solute complex. Thus, the solute complex can be viewed as a probe charge that does not impact the potential $\phi_s(x)$. The work required to move the solute complex with charge ze from the bulk solution at $\phi_s(\infty) = 0$ to a point at a distance x from the electrode surface with potential $\phi_s(x)$ is $ze\phi_s(x)$. Adding this electrostatic work term to the energy of the reduced solvated solute complex in bulk solution, the total energy of the system in its initial electronic state is given by

$$\mathcal{E}_i(r_p, R, \xi|x) = \mathcal{E}_I^0(r_p, R, \xi) + ze\phi_s(x) \tag{7}$$

For simplicity, the total electronic energy of the electrode is assumed to be a constant set to zero in the initial electronic state. We are assuming that electron exchange between the solute complex in solution and the electrode is not coupled to electronic excitations in the electrode.

In the final electronic state, $|\Psi_f\rangle$, the solute complex is in its oxidized form, SC^+, and the transferred electron is in the one-electron level $|\psi_m\rangle$ of the electrode with energy ϵ_m relative to the Fermi energy, μ_M. As defined previously, the oxidized solvated solute complex has energy $\mathcal{E}_{II}^0(r_p, R, \xi)$ in bulk solution. The total energy of the system in its final electronic state is given by

$$\mathcal{E}_f(r_p, R, \xi|x) = \mathcal{E}_{II}^0(r_p, R, \xi) + (z+1)e\phi_s(x) + \epsilon_m + \mu_M - e\phi_M \tag{8}$$

where $(z+1)e$ is the total charge of the oxidized complex, and ϕ_M is the previously defined inner potential of the electrode.

Given these definitions, we can calculate the proton vibrational states for the initial and final diabatic electronic states. These vibrational states are calculated by solving the Schrödinger equations for the proton motion when the solvated solute complex is in its initial (SC) or final (SC^+) electronic state:

$$\begin{aligned}[\hat{T}_p + \mathcal{E}_I^0(r_p, R, \xi)]\ \chi_\mu^i(r_p|R, \xi) &= U_\mu^I(R, \xi)\ \chi_\mu^i(r_p|R, \xi) \\ [\hat{T}_p + \mathcal{E}_{II}^0(r_p, R, \xi)]\ \chi_\nu^f(r_p|R, \xi) &= U_\nu^{II}(R, \xi)\ \chi_\nu^f(r_p|R, \xi)\end{aligned} \tag{9}$$

where χ_μ^i and χ_ν^f are the initial and final proton vibrational wave functions. This procedure, often denoted the double adiabatic approximation for the proton motion,[58] yields two sets of vibronic surfaces, $\mathcal{U}_\mu^i$ and $\mathcal{U}_\nu^f$, that depend explicitly on the proton donor−acceptor distance R and the solvent coordinates ξ:

$$\begin{aligned}\mathcal{U}_\mu^i(R, \xi|x) &= U_\mu^I(R, \xi) + ze\phi_s(x) \\ \mathcal{U}_\nu^f(R, \xi|x) &= U_\nu^{II}(R, \xi) + (z+1)e\phi_s(x) + \epsilon_m + \mu_M - e\phi_M\end{aligned} \tag{10}$$

Although the product vibronic surface $\mathcal{U}_\nu^f$ depends on the index m associated with the metal one-electron energy level ϵ_m, we omit this dependence for notational simplicity.

Figure 2 depicts one-dimensional slices of these intersecting multidimensional surfaces along a collective solvent coordinate for a given pair of surfaces, $\mathcal{U}_\mu^i$ and $\mathcal{U}_\nu^f$. Here, the product vibronic surface, $\mathcal{U}_\nu^f$, is represented by a continuum of surfaces originating from the electronic states in the conduction band of the metal electrode. As shown in Figure 2, in the initial electronic state, the proton potential is asymmetric with the donor well lower in energy, and the ground proton vibrational state is localized on the proton donor. In contrast, in the final electronic state, the proton potential is asymmetric with the acceptor well lower in energy, and the ground proton vibrational state is localized on the proton acceptor.

The next step is the construction of effective channel Hamiltonians for the initial and final states:

$$\begin{aligned}\hat{\mathcal{H}}_\mu^i &= \hat{T}_R + \hat{T}_\xi + \mathcal{U}_\mu^i(R, \xi|x) \\ \hat{\mathcal{H}}_\nu^f &= \hat{T}_R + \hat{T}_\xi + \mathcal{U}_\nu^f(R, \xi|x)\end{aligned} \tag{11}$$

These channel Hamiltonians enable the calculation of two sets of quantum vibrational states for the R mode and the solvent modes, ξ:

$$\begin{aligned}\hat{\mathcal{H}}_\mu^i\ \zeta_l^{i\mu}(R, \xi|x) &= E_l^{i\mu}(x)\ \zeta_l^{i\mu}(R, \xi|x) \\ \hat{\mathcal{H}}_\nu^f\ \zeta_n^{f\nu}(R, \xi|x) &= E_n^{f\nu}(x)\ \zeta_n^{f\nu}(R, \xi|x)\end{aligned} \tag{12}$$

The total vibronic wave functions for the system in its initial and final states are constructed as products of the electronic and vibrational wave functions. The products for the initial and

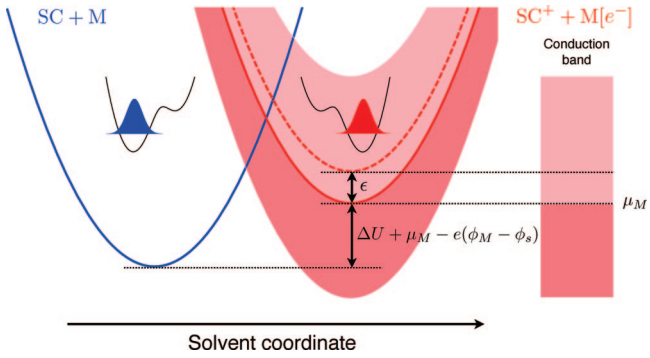

Figure 2. Free energy curves for the electrochemical PCET reaction as functions of the collective solvent coordinate. Only the ground reactant and product vibronic states are shown. The reactant free energy curve on the left (blue) corresponds to the reduced form of the solute complex, SC, in solution and the metal electrode, M, in its initial electronic state, which is assumed to have a constant energy set to zero. The continuum of curves on the right (red) represents the oxidized solute complex, SC^+, and the metal electrode, $M[e^-]$, with an additional electron occupying one of the one-electron states in the conduction band of the metal. The initial and final electronic states are the same except for the occupation of a one-electron state localized on the solute complex for the initial state and on the metal electrode for the final state. The solid red curve on the right corresponds to the one-electron metal state at the Fermi level of the electrode (μ_M), and the dashed red curve on the right corresponds to the one-electron metal state with energy ϵ relative to the Fermi level. In the anodic (oxidation) process, the reaction occurs via nonadiabatic transitions from the left curve to any of the curves in the product continuum. The transitions occur at the intersection points between the blue and red curves. The reaction free energy for each of these transitions is the sum of the intrinsic free energy difference, ΔU; the Fermi level of the electrode, μ_M; the energy, ϵ, of the accepting one-electron state of the electrode; and $-e(\phi_M - \phi_s)$, which arises from the difference between the electrostatic potentials in the metal and in solution at the solute complex. The proton potential energy profiles as functions of the proton coordinate, r_p, and the associated ground-state proton vibrational wave functions are also shown for the reactant and product vibronic states.

final states are denoted as $|\Psi_i\, \chi_\mu^i\, \zeta_l^{i\mu}\rangle$ and $|\Psi_f\, \chi_\nu^f\, \zeta_n^{f\nu}\rangle$, respectively.

B. Nonadiabatic Transition Probabilities and Rate Constants. Nonadiabatic transitions between the eigenstates of the channel Hamiltonians occur due to the perturbation term $\hat{V}$. We assume that the matrix elements of this perturbation between the initial and final vibronic states are small compared to the thermal energy k_BT, so first-order, time-dependent perturbation theory can be used to calculate the transition probabilities. In this case, the rate constant for quantum transitions from the set $|\Psi_i\, \chi_\mu^i\, \zeta_l^{i\mu}\rangle$ to the set $|\Psi_f\, \chi_\nu^f\, \zeta_n^{f\nu}\rangle$ is given by Fermi's Golden Rule:[41]

$$W_{i\to f} = \frac{2\pi}{\hbar}\sum_{\mu,l} P_{\mu l}^{(i)} \sum_{\nu,n} \left|\langle \xi_n^{f\nu}\, \chi_\nu^f\, \Psi_f|\hat{V}|\Psi_i\, \chi_\mu^i\, \zeta_l^{i\mu}\rangle\right|^2 \delta(E_l^{i\mu} - E_n^{f\nu}) \tag{13}$$

where $P_{\mu l}^{(i)}$ are the Boltzmann probabilities for the reactant states, which are assumed to be in thermal equilibrium, leading to the expression

$$P_{\mu l}^{(i)} = \frac{e^{-\beta E^{i\mu}_l}}{\sum_{n,\nu} e^{-\beta E_n^{i\nu}}} \tag{14}$$

In eq 13, the summations are over the proton vibrational states (μ, ν) and the solvent/R-mode vibrational states (l, n). The delta function ensures energy conservation during the transition from the initial to the final state.

The rate constant can be expressed in terms of the Heisenberg time evolution of the nonadiabatic couplings and the energy gaps, governed by the reactant channel Hamiltonians, $\hat{\mathscr{H}}_\mu^i$

$$\hat{V}_{\mu\nu}^{(m)}(t) = e^{i\hat{\mathscr{H}}_\mu^i t/\hbar}\, \hat{V}_{\mu\nu}^{(m)}(x, R, \xi) e^{-i\hat{\mathscr{H}}_\mu^i t/\hbar} \tag{15}$$

$$\Delta\hat{\mathscr{H}}_{\mu\nu}^{(m)}(t) = e^{i\hat{\mathscr{H}}_\mu^i t/\hbar}(\hat{\mathscr{H}}_\nu^f - \hat{\mathscr{H}}_\mu^i) e^{-i\hat{\mathscr{H}}_\mu^i t/\hbar} \tag{16}$$

Note that the nonadiabatic coupling, $\hat{V}_{\mu\nu}^{(m)}(x, R, \xi) = \langle \chi_\nu^f \Psi_f|\hat{V}|\Psi_i\, \chi_\mu^i\rangle$, depends on the location x of the solute complex and the state $|\psi_m\rangle$ of the transferred electron in the metal. For notational simplicity, the dependence of $\hat{\mathscr{H}}_\nu^f$ on the index m associated with the metal state $|\psi_m\rangle$ is omitted.

The transition probability per unit time is expressed as the time integral of the probability flux correlation function, $j_{\mu\nu}(t)$:[50,51]

$$W_{i\to f} = \frac{1}{\hbar^2}\sum_{\mu,\nu} P_\mu^{(i)} \int_{-\infty}^{\infty} j_{\mu\nu}(t)\, dt \tag{17}$$

where

$$j_{\mu\nu}(t) = \left\langle \hat{V}_{\mu\nu}^{(m)}(0)\, \exp_{(-)}\left[\frac{i}{\hbar}\int_0^t d\tau\, \Delta\hat{\mathscr{H}}_{\mu\nu}^{(m)}(\tau)\right]\hat{V}_{\mu\nu}^{(m)}(t)\right\rangle_{\{i\mu\}} \tag{18}$$

The thermodynamic average is defined as

$$\langle \cdots \rangle_{\{i\mu\}} = Tr(e^{-\beta\hat{\mathscr{H}}_\mu^i} \cdots)/Tr(e^{-\beta\hat{\mathscr{H}}_\mu^i}) \tag{19}$$

and $P_\mu^{(i)}$ are the Boltzmann weights for the reactant electron−proton vibronic states.

The Heisenberg time evolution of the energy gap can be approximated in terms of the time evolution of the R mode and the solvent modes on the reactant electron−proton vibronic surface:

$$\Delta\hat{\mathscr{H}}_{\mu\nu}^{(m)}(\tau) = \mathscr{U}_\nu^f(\hat{R}(\tau), \hat{\xi}(\tau)|x) - \mathscr{U}_\mu^i(\hat{R}(\tau), \hat{\xi}(\tau)|x) \tag{20}$$

Analogous to homogeneous PCET, the nonadiabatic coupling is assumed to have an exponential dependence on the proton donor−acceptor distance, R.[42,53] Invoking the Condon approximation with respect to the solvent modes ξ, the Heisenberg time-evolved coupling is approximated as

$$\hat{V}_{\mu\nu}^{(m)}(t) = V_{\mu\nu}(x, \epsilon_m, \bar{R}_\mu) e^{-\alpha_{\mu\nu}(\hat{R}(t) - \bar{R}_\mu)} = \tilde{V}_{\mu\nu}(x, \epsilon_m) e^{-\alpha_{\mu\nu}(\hat{R}(t) - \bar{R}_\mu)} \tag{21}$$

Here $V_{\mu\nu}(x, \epsilon_m, \bar{R}_\mu)$ is the nonadiabatic coupling between reactant and product electron−proton vibronic states μ and ν, respectively, when the solute complex is a distance x from the electrode, the proton donor−acceptor distance is $\bar{R}_\mu$, and the electron is being transferred to a state with energy ϵ_m in the electrode. According to the Condon approximation, this coupling is independent of the solvent modes. For notational convenience, we define $\tilde{V}_{\mu\nu}(x, \epsilon_m)$ to be evaluated at the equilibrium value $\bar{R}_\mu$ of the R coordinate on the reactant vibronic surface μ.

Linear Approximation for the *R* Mode. To approximate the time evolution of the energy gap given in eq 20, we expand the energy gap to linear order in the R coordinate around its equilibrium value, $\bar{R}_\mu$, on the reactant surface. The resulting time evolution of the energy gap is given by

$$\Delta\hat{\mathscr{H}}_{\mu\nu}^{(m)}(\tau) = \Delta U_{\mu\nu}(\bar{R}_\mu, \hat{\xi}(\tau)) + D_{\mu\nu}(\hat{\xi}(\tau))\delta\hat{R}_\mu(\tau) + e\phi_s(x) + \epsilon_m + \mu_M - e\phi_M \tag{22}$$

where

$$\Delta U_{\mu\nu}(\bar{R}_\mu, \hat{\xi}(\tau)) = U_\nu^{\mathrm{II}}(\bar{R}_\mu, \hat{\xi}(\tau)) - U_\mu^{\mathrm{I}}(\bar{R}_\mu, \hat{\xi}(\tau))$$
$$D_{\mu\nu}(\hat{\xi}(\tau)) = \frac{\partial \Delta U_{\mu\nu}(R, \hat{\xi}(\tau))}{\partial R}\Big|_{R=\bar{R}_\mu} \quad (23)$$
$$\delta\hat{R}_\mu(\tau) = \hat{R}(\tau) - \bar{R}_\mu$$

We also introduce the following time correlation functions for the quantities defined in eq 23

$$\begin{aligned} C_R(t) &= \langle \delta\hat{R}_\mu(0)\, \delta\hat{R}_\mu(t)\rangle \\ C_U(t) &= \langle \Delta U_{\mu\nu}(0)\, \Delta U_{\mu\nu}(t)\rangle \\ C_D(t) &= \langle D_{\mu\nu}(0)\, D_{\mu\nu}(t)\rangle \end{aligned} \quad (24)$$

with

$$\Delta U_{\mu\nu}(t) \equiv \Delta U_{\mu\nu}(\bar{R}_\mu, \hat{\xi}(t)); \quad D_{\mu\nu}(t) \equiv D_{\mu\nu}(\hat{\xi}(t)) \quad (25)$$

Using Kubo's cumulant expansion,[59] the probability flux correlation function reduces to the familiar form[42,51,52]

$$\begin{aligned} j_{\mu\nu}(t) = &\left|\tilde{V}_{\mu\nu}(x, \epsilon_m)\right|^2 \times \\ &\exp\left[\alpha_{\mu\nu}^2 (C_R(0) + C_R(t)) - \frac{2i\alpha_{\mu\nu}}{\hbar}\langle D_{\mu\nu}\rangle \int_0^t \mathrm{d}\tau\, C_R(\tau)\right] \times \\ &\exp\left[\frac{it}{\hbar}(\langle \Delta U_{\mu\nu}(0)\rangle + e\phi_s(x) - e\phi_M + \epsilon_m + \mu_M)\right] \times \\ &\exp\left[-\frac{1}{\hbar^2}\int_0^t \mathrm{d}\tau_1 \int_0^{\tau_1} \mathrm{d}\tau_2 (C_U(\tau_1 - \tau_2) + \right. \\ &\left. C_D(\tau_1 - \tau_2) C_R(\tau_1 - \tau_2))\right] \end{aligned} \quad (26)$$

where we have neglected the dynamical coupling between the R mode and solvent modes.

$$\begin{aligned} \langle D_{\mu\nu}(\tau)\, \delta\hat{R}_\mu(\tau)\rangle &\approx \langle D_{\mu\nu}\rangle \langle \delta\hat{R}_\mu\rangle \approx 0 \\ \langle \delta\hat{R}_\mu(\tau)\, U_{\mu\nu}(\tau)\rangle &\approx \langle \delta\hat{R}_\mu\rangle \langle U_{\mu\nu}\rangle \approx 0 \end{aligned} \quad (27)$$

In these equations, the thermodynamic averages are calculated using the initial state Hamiltonian

$$\hat{\mathscr{H}}_\mu^{\mathrm{i}} = \hat{T}_R + \hat{T}_\xi + U_\mu^{\mathrm{I}}(R, \xi) + ze\phi_s(x) \quad (28)$$

The expression for the probability flux correlation function in eq 26 has a form similar to the expression derived previously for homogeneous PCET,[42,60] except for the terms $e\phi_s(x) - e\phi_M + \epsilon_m + \mu_M$, which correspond to the effects of the metal electrode on the energy gap. In addition, the electrochemical probability flux correlation function, and the vibronic coupling in particular, depend on the distance x between the electrode and the solute complex and the energy level ϵ_m of the transferring electron in the electrode. The integration over these variables is discussed below for the analytical expressions of the transition probabilities. Here we point out that the probability flux correlation function in eq 26 and, thus, the nonadiabatic transition probabilities can be evaluated using correlation functions extracted from molecular dynamics trajectories for the system moving on the reactant vibronic energy surface. At ambient temperatures and low characteristic frequencies for the R mode and solvent modes, the quantum effects on the dynamics are negligible, and the correlation functions can be calculated from classical trajectories. We have used this approach to study homogeneous PCET reactions in solution and proteins.[60,61] The effects of the metal electrode and electrostatic potentials can be incorporated into molecular dynamics simulations using methodology previously applied to electrochemical ET.[62−67]

Harmonic Approximation. Analogous to the case of homogeneous PCET,[42] analytical expressions for the nonadiabatic transition probabilities in electrochemical PCET systems can be derived within the harmonic approximation for the effective solvent modes $\mathbf{q} \equiv \{q_k\}$ and the R mode. Note that these effective solvent modes do not correspond directly to the solvent coordinates but, rather, correspond to the Fourier components of the inertial polarization field of the solvent.[68] In this approximation, the reactant and product vibronic surfaces $U_\mu^{\mathrm{I}}(R, \mathbf{q})$ and $U_\nu^{\mathrm{II}}(R, \mathbf{q})$ are assumed to be multidimensional paraboloids with minima at $(\bar{R}_\mu, \bar{\mathbf{q}}_\mu)$ and $(\bar{R}_\nu, \bar{\mathbf{q}}_\nu)$, respectively, so the analytical expressions for the position time correlation functions of harmonic oscillators can be used. In this case, we obtain the following expression for the transition probability (per unit time) of PCET from the reduced solute complex (SC) located at a distance x from the electrode surface to a one-electron state $|\psi_m\rangle$ in the electrode with energy ϵ_m:

$$\begin{aligned} W_{\mathrm{SC}\to\mathrm{M}}(x, \epsilon_m) = &\frac{1}{\hbar^2}\sum_{\mu,\nu} P_\mu^{(\mathrm{i})} \left|\tilde{V}_{\mu\nu}(x, \epsilon_m)\right|^2 \times \\ &\exp\left[\frac{2\lambda_{\mu\nu}^{(\alpha)}\zeta_R}{\hbar\Omega_R}\right] \int_{-\infty}^{\infty} \mathrm{d}t \exp\left[\frac{it}{\hbar}(\Delta G_{\mu\nu}(x, \epsilon_m) + \lambda_s)\right] \times \\ &\exp[p(\cos\Omega_R t - 1) + iq \sin\Omega_R t] \times \\ &\exp\left[\sum_k \frac{d_k}{\hbar\omega_k}[\zeta_k(\cos\omega_k t - 1) + i(\sin\omega_k t - \omega_k t)]\right] \end{aligned} \quad (29)$$

Here, Ω_R and ω_k are the frequencies of the R mode and the solvent modes, respectively, with corresponding masses m_R and m_k. Moreover, $\lambda_R = m_R\Omega_R^2\, \delta R^2/2$ and $\lambda_s = \sum_k d_k = \sum_k m_k\omega_k^2\, \delta q_k^2/2$ are the R mode and solvent reorganization energies, respectively, originating from the shifts of the equilibrium positions $\delta R = \bar{R}_\nu - \bar{R}_\mu$ and $\delta\mathbf{q} = \bar{\mathbf{q}}_\nu - \bar{\mathbf{q}}_\mu$, which are assumed to be the same for all pairs of reactant and product vibronic states. Furthermore, $\lambda_{\mu\nu}^{(\alpha)} = \hbar^2\alpha_{\mu\nu}^2/2m_R$ is the coupling reorganization energy characterizing the strength of the R dependence of the nonadiabatic couplings for a given pair of reactant and product vibronic states. The Boltzmann probabilities, $P_\mu^{(\mathrm{i})}$, for the initial vibronic states are given by

$$P_\mu^{(\mathrm{i})} = \frac{\mathrm{e}^{-\beta\mathscr{U}_\mu^{\mathrm{i}}(\bar{R}_\mu, \bar{\mathbf{q}}_\mu | x)}}{\sum_k \mathrm{e}^{-\beta\mathscr{U}_k^{\mathrm{i}}(\bar{R}_k, \bar{\mathbf{q}}_k | x)}} \quad (30)$$

The additional parameters are defined as

$$\begin{aligned} p &= \zeta_R \frac{\lambda_{\mu\nu}^{(\alpha)} + \lambda_R}{\hbar\Omega_R} + \alpha_{\mu\nu}\, \delta R \\ q &= \frac{\lambda_{\mu\nu}^{(\alpha)} + \lambda_R}{\hbar\Omega_R} + \zeta_R\alpha_{\mu\nu}\, \delta R \\ \zeta_R &= \coth\left(\frac{\beta\hbar\Omega_R}{2}\right); \quad \zeta_k = \coth\left(\frac{\beta\hbar\omega_k}{2}\right) \end{aligned} \quad (31)$$

Finally, the free energy difference $\Delta G_{\mu\nu}(x, \epsilon_m)$ for the pair of reactant and product vibronic states μ and ν is the free energy difference between the minima of the corresponding electron−proton vibronic surfaces plus additional terms, depending on the electrostatic potentials in solution and in the metal electrode, as well as the energy level of the transferring electron in the electrode:

$$\Delta G_{\mu\nu}(x, \epsilon_m) = \Delta U_{\mu\nu} + \epsilon_m + \mu_M - \mathrm{e}(\phi_M - \phi_s(x)) \quad (32)$$

Here, the intrinsic free energy difference

$$\Delta U_{\mu\nu} = U_{\nu}^{\mathrm{II}}(\bar{R}_{\nu}, \bar{\mathbf{q}}_{\nu}) - U_{\mu}^{\mathrm{I}}(\bar{R}_{\mu}, \bar{\mathbf{q}}_{\mu}) \tag{33}$$

is defined as the difference between the minima of the vibronic surfaces for the oxidized and reduced forms of the solute complex in bulk solution (i.e., in the absence of the electrode). These quantities are depicted in Figure 2.

The expression given in eq 29 can be further simplified in the high temperature limit for the R mode and the solvent modes. The expressions for the low-temperature limit for the R mode are given in the Appendix. The high-temperature (low-frequency) limit for the R mode corresponds to $\beta\hbar\Omega_R \ll 1$. The high-temperature limit for the solvent modes corresponds to $\beta\hbar\omega_c \ll 1$, where ω_c is the cutoff frequency for the solvent modes. In this limit, we can use a short time approximation, provided that the solvent reorganization energy, λ_s, is large enough for the strong solvation condition to be satisfied:[69,70]

$$\sqrt{\frac{2\lambda_s}{\beta\hbar^2\omega_c^2}} \gg 1 \tag{34}$$

The short time approximation is equivalent to the assumption that the dynamics of the solvent fluctuations are fast on the time scale of the coherent nonadiabatic transitions. In this limit, the time decay of the probability flux correlation function is dominated by the strong damping term originating from the equilibrium solvent fluctuations, and we can retain only terms up to second order in the expansions of the periodic time-dependent functions in eq 29 around $t = 0$. This approximation enables the analytical integration of eq 29 over time.

The resulting analytical expression for the oxidation transition probability is:

$$W_{\mathrm{SC}\rightarrow\mathrm{M}}(x,\epsilon_m) = \frac{1}{\hbar}\sum_{\mu,\nu} P_{\mu}^{(\mathrm{i})}\left|\tilde{V}_{\mu\nu}(x,\epsilon_m)\right|^2 \times \exp\left[\frac{4\lambda_{\mu\nu}^{(\alpha)}}{\beta\hbar^2\Omega_R^2}\right]\sqrt{\frac{\pi\beta}{\Lambda_{\mu\nu}}}\exp\left[\frac{-\beta(\Delta G_{\mu\nu}(x,\epsilon_m)+\Lambda_{\mu\nu}^{+})^2}{4\Lambda_{\mu\nu}}\right] \tag{35}$$

where the total and adjusted reorganization energies are given by

$$\begin{aligned}\Lambda_{\mu\nu} &= \lambda_s + \lambda_R + \lambda_{\mu\nu}^{(\alpha)}\\ \Lambda_{\mu\nu}^{+} &= \Lambda_{\mu\nu} + \frac{2\alpha_{\mu\nu}\,\delta R}{\beta}\end{aligned} \tag{36}$$

Similarly, the transition probability of PCET from the one-electron state $|\psi_m\rangle$ with energy ϵ_m in the metal electrode to the oxidized form of the solute complex (SC^+) located at a distance x from the electrode surface is given by

$$\begin{aligned}&W_{\mathrm{M}\rightarrow\mathrm{SC}^+}(x,\epsilon_m) =\\ &\frac{1}{\hbar^2}\sum_{\mu,\nu} P_{\nu}^{(\mathrm{f})}\left|\tilde{V}_{\mu\nu}(x,\epsilon_m)\right|^2 \exp\left[\frac{2\lambda_{\mu\nu}^{(\alpha)}\zeta_R}{\hbar\Omega_R} - 2\alpha_{\mu\nu}\delta R\right]\times\\ &\int_{-\infty}^{\infty} \mathrm{d}t \exp\left[\frac{it}{\hbar}(-\Delta G_{\mu\nu}(x,\epsilon_m)+\lambda_s)\right]\times\\ &\exp[p'(\cos\Omega_R t - 1) + iq'\sin\Omega_R t]\times\\ &\exp\left[\sum_k \frac{\mathrm{d}_k}{\hbar\omega_k}(\zeta_k(\cos\omega_k t - 1) + i(\sin\omega_k t - \omega_k t))\right]\end{aligned} \tag{37}$$

where the parameters p' and q' are given by

$$\begin{aligned}p' &= \zeta_R\frac{\lambda_{\mu\nu}^{(\alpha)}+\lambda_R}{\hbar\Omega_R} - \alpha_{\mu\nu}\delta R\\ q' &= \frac{\lambda_{\mu\nu}^{(\alpha)}+\lambda_R}{\hbar\Omega_R} - \zeta_R\alpha_{\mu\nu}\delta R\end{aligned} \tag{38}$$

The corresponding closed analytical expression in the high-temperature limit for the R mode and the solvent modes is

$$W_{\mathrm{M}\rightarrow\mathrm{SC}^+}(x,\epsilon_m) = \frac{1}{\hbar}\sum_{\nu,\mu} P_{\nu}^{(\mathrm{f})}\left|\tilde{V}_{\mu\nu}(x,\epsilon_m)\right|^2 \exp\left[\frac{4\lambda_{\mu\nu}^{(\alpha)}}{\beta\hbar^2{\Omega_R}^2} - 2\alpha_{\mu\nu}\delta R\right]\times \sqrt{\frac{\pi\beta}{\Lambda_{\mu\nu}}}\exp\left[\frac{-\beta(-\Delta G_{\mu\nu}(x,\epsilon_m)+\Lambda_{\mu\nu}^{-})^2}{4\Lambda_{\mu\nu}}\right] \tag{39}$$

where the adjusted reorganization energy is given by

$$\Lambda_{\mu\nu}^{-} = \Lambda_{\mu\nu} - \frac{2\alpha_{\mu\nu}\,\delta R}{\beta} \tag{40}$$

and the Boltzmann probability, $P_{\nu}^{(\mathrm{f})}$, for the vibronic states of the oxidized complex SC^+ is given by the analog of eq 30.

The factor $\exp[-2\alpha_{\mu\nu}\,\delta R]$ in eqs 37 and 39 arises from the relation between the nonadiabatic vibronic coupling at $\bar{R}_{\nu}$ and $\bar{R}_{\mu}$. As seen from eq 21,

$$V_{\mu\nu}(x,\epsilon_m,\bar{R}_{\nu}) = V_{\mu\nu}(x,\epsilon_m,\bar{R}_{\mu})\mathrm{e}^{-\alpha_{\mu\nu}\delta R} \tag{41}$$

For notational convenience, we have defined $\tilde{V}_{\mu\nu}(x,\epsilon_m)$ to be evaluated at $\bar{R}_{\mu}$, which corresponds to the equilibrium proton donor−acceptor distance of the reduced solute complex, for both the forward and reverse reactions. Similarly, $\delta R = \bar{R}_{\nu} - \bar{R}_{\mu}$ is defined to be the difference between the oxidized and reduced solute complex equilibrium proton donor−acceptor distances for both the forward and reverse reactions. These definitions are used consistently in all of the expressions for transition probabilities, rate constants, and current densities.

The total first order rate constants are obtained by summing over all of the available metal states weighted by the Fermi distribution, $f(\epsilon_m)$, given in eq 2. Introducing the density of states $\rho(\epsilon)$ in the electrode, we can replace the summation with integration over the entire conduction band. The resulting expressions for the oxidation and reduction rate constants are

$$\begin{aligned}k_{\mathrm{SC}\rightarrow\mathrm{M}}(x) &= \int \mathrm{d}\epsilon\,[1-f(\epsilon)]\,\rho(\epsilon)\,W_{\mathrm{SC}\rightarrow\mathrm{M}}(x,\epsilon)\\ k_{\mathrm{M}\rightarrow\mathrm{SC}^+}(x) &= \int \mathrm{d}\epsilon\, f(\epsilon)\,\rho(\epsilon)\,W_{\mathrm{M}\rightarrow\mathrm{SC}^+}(x,\epsilon)\end{aligned} \tag{42}$$

C. Current Densities. Using the expressions for the first-order rate constants derived in the previous subsection, we can calculate the current densities for the oxidation and reduction PCET reactions at the metal electrode. Current density is an important quantity that is directly measured in electrochemical experiments. Anodic (j_a) and cathodic (j_c) current densities are defined for oxidation and reduction processes, respectively, and are obtained by integrating the rates over the distance x to the electrode surface,

$$\begin{aligned}j_a &= F\int_{x_H}^{\infty}\mathrm{d}x\,C_{\mathrm{SC}}(x)\,k_{\mathrm{SC}\rightarrow\mathrm{M}}(x)\\ j_c &= F\int_{x_H}^{\infty}\mathrm{d}x\,C_{\mathrm{SC}^+}(x)\,k_{\mathrm{M}\rightarrow\mathrm{SC}^+}(x)\end{aligned} \tag{43}$$

where F is the Faraday constant, $C_{\mathrm{SC}}(x)$ and $C_{\mathrm{SC}^+}(x)$ are the molar concentrations of the reduced and oxidized solute complexes, respectively, at a distance x from the electrode surface, and x_H was previously defined to be the distance

corresponding to the outer Helmholtz plane. The first-order oxidation and reduction rate constants are given in eq 42.

To facilitate the integration over x, we assume that the rate constants decrease exponentially with the distance x. This assumption can be justified by noting that the nonadiabatic transition probabilities are proportional to the square of the nonadiabatic vibronic coupling $\tilde{V}_{\mu\nu}(x,\epsilon)$. For electronically nonadiabatic PCET reactions, the vibronic coupling can be approximated as a product of the electronic coupling $V^{el}(x,\epsilon)$ and the overlap integral, $S_{\mu\nu}$, of the reactant and product proton vibrational wave functions.[71,72] The overlap integrals $S_{\mu\nu}$ do not depend significantly on the distance x or the energy ϵ and are assumed to be determined entirely by the properties of the proton transfer interface. Furthermore, typically the electronic coupling is assumed to decrease exponentially with x. Thus, the x-dependence of the rate constants can be approximated as follows:[73]

$$\begin{aligned} k_{SC\rightarrow M}(x) &= k_{SC\rightarrow M}(x_H)\, e^{-\beta'(x-x_H)} \\ k_{M\rightarrow SC^+}(x) &= k_{M\rightarrow SC^+}(x_H)\, e^{-\beta'(x-x_H)} \end{aligned} \tag{44}$$

where β' is typically $1-3$ Å^{-1}. Here, we are assuming that the exponential factor β' does not vary significantly with the metal one-electron energy level, ϵ.

To evaluate the integrals over the distance x in eq 43, we also need to make assumptions about the dependence of the solute complex concentration on the distance x. For simplicity, we assume that the electron transfer processes at the electrode surface are much slower than the diffusion processes in solution, so the equilibrium distribution of solute complexes in the diffuse layer and beyond is maintained during the reaction. This assumption holds for low currents and a relatively low concentration of solute complexes in solution. In this case, the concentrations of the reduced and oxidized solute complexes in the diffuse layer just outside the outer Helmholtz plane and beyond are obtained from the Boltzmann distribution,

$$\begin{aligned} C_{SC}(x) &= C^0_{SC}\exp[-\beta z e\phi_s(x)] \\ C_{SC^+}(x) &= C^0_{SC^+}\exp[-\beta(z+1)e\phi_s(x)] \end{aligned} \tag{45}$$

where C^0_{SC} and $C^0_{SC^+}$ are the bulk concentrations and $\phi_s(x)$ is the previously defined solution potential at a distance x from the electrode relative to the potential in bulk solution at $x \rightarrow \infty$.

According to the Gouy−Chapman−Stern model of the double layer,[74,75] the potential $\phi_s(x)$ in the diffuse layer is obtained from the equation

$$\frac{\tanh[z_{el}\beta e\phi_s(x)/4]}{\tanh[z_{el}\beta e\psi/4]} = e^{-\kappa(x-x_H)} \tag{46}$$

Here, $\psi = \phi_s(x_H)$ is the potential at the OHP, z_{el} is the magnitude of the charge on each electrolyte ion, and κ^{-1} is the Debye length that characterizes the thickness of the diffuse layer and varies as $I_{el}^{-1/2}$, where I_{el} is the ionic strength of the supporting electrolyte. In this model, the electrolytic solution is assumed to contain ions of charge $\pm z_{el}e$, with equal bulk concentrations of cations and anions. The contribution of the solute complex, which has charge ze or $(z+1)e$ in the reduced or oxidized state, respectively, to the potential $\phi_s(x)$ is neglected.

Within this model, the integrals in eq 43 can be evaluated in two limits.[47,73] At low concentrations of the electrolyte, the thickness of the diffuse layer is larger than the characteristic length of the decay of the transition probability. In this case, $\beta' \gg \kappa$, and the current is dominated by PCET occurring at the outer Helmholtz plane, x_H. The current densities in this limit are given by

$$\begin{aligned} j_a &= FC^0_{SC}\frac{k_{SC\rightarrow M}(x_H)}{\beta'}e^{-z\beta e\psi} \\ j_c &= FC^0_{SC^+}\frac{k_{M\rightarrow SC^+}(x_H)}{\beta'}e^{-(z+1)\beta e\psi} \end{aligned} \tag{47}$$

where the exponential factors represent the double layer corrections depending on the potential at the outer Helmholtz plane. At higher electrolyte concentrations, $\beta' \ll \kappa$, and the current is dominated by PCET occurring outside the very thin diffuse layer.[47] In this case, the double layer corrections can be neglected, and the current densities are given by eqs 47 with $\psi = 0$. The remainder of the derivations will be based on the expressions in eqs 47, which are valid at low concentrations of the supporting electrolyte when $\beta' \gg \kappa$. All of the results can be easily modified for high electrolyte concentrations by setting $\psi = 0$.

The remainder of this subsection focuses on the derivation of the total current density measured in the electrochemical cell as a function of the external voltage applied to the working metal electrode. Following the procedure proposed by Levich,[12] we can express the total current density, $j = j_a - j_c$, in terms of the transition probabilities for the oxidation process. Using the expressions given in eqs 35, 39, 42, and 47, the total current density can be expressed as

$$\begin{aligned} j = \frac{F}{\beta'\hbar}C^0_{SC}e^{-z\beta e\psi}\int d\epsilon\,(1-f(\epsilon))\,\rho(\epsilon)\sum_{\mu,\nu}P^{(i)}_\mu \times \\ \left|\tilde{V}_{\mu\nu}(x_H,\epsilon)\right|^2\sqrt{\frac{\pi\beta}{\Lambda_{\mu\nu}}}\exp\left[\frac{4\lambda^{(\alpha)}_{\mu\nu}}{\beta\hbar^2\Omega_R{}^2}\right]\times \\ \exp\left[\frac{-\beta(\Delta G_{\mu\nu}(x_H,\epsilon)+\Lambda^+_{\mu\nu})^2}{4\Lambda_{\mu\nu}}\right]\times \\ \left\{1-\frac{C^0_{SC^+}}{C^0_{SC}}\frac{Q^I}{Q^{II}}\exp[-\beta eE+\beta\mu_M]\right\} \end{aligned} \tag{48}$$

where $E \equiv \phi_M$ is the electrode potential;

$$Q^I = \sum_\mu e^{-\beta U^I_\mu(\bar{R}_\mu,\bar{q}_\mu)};\quad Q^{II} = \sum_\nu e^{-\beta U^{II}_\nu(\bar{R}_\nu,\bar{q}_\nu)} \tag{49}$$

are the total partition functions of the reduced and oxidized solute complexes, respectively, in bulk solution; and the Boltzmann probability $P^{(i)}_\mu$ is given by eq 30 evaluated at $x = x_H$. Note that the derivation of eq 48 used the Fermi distribution function given in eq 2 and would be problematic if the Fermi distribution were approximated as a Heaviside step function $\Theta(\epsilon)$ due to the divergence of the ratio $\Theta(\epsilon)/(1-\Theta(\epsilon))$. Therefore, the approximation of the Fermi distribution by the Heaviside step function to enable the analytical evaluation of the integral over ϵ in eq 48 and subsequent equations would be inconsistent and would lead to the violation of detailed balance. For this reason, we use the Fermi distribution function given in eq 2 throughout this paper.

At equilibrium with potential $E = E_{eq}$, the total current is zero, and the ratio of equilibrium concentrations is determined by the Nernst equation,

$$\left[\frac{C^0_{SC}}{C^0_{SC^+}}\right]_{eq} = e^{-\beta e(E_{eq}-E^0)} \tag{50}$$

where E^0 is the formal electrode potential. Substituting the equilibrium ratio of concentrations into eq 48, setting the expression in curly brackets to zero, and using eq 50, we obtain

the following relation for the formal electrode potential, E^0, for this PCET reaction system:

$$eE^0 = \mu_M + \frac{1}{\beta}\ln\frac{Q^I}{Q^{II}} \tag{51}$$

Using this relation, we can now express the total nonequilibrium current density in terms of the overpotential, $\eta = E - E^0$ as

$$j(\eta) = \frac{F}{\beta'\hbar}C^0_{SC}e^{-z\beta e\psi}\int d\epsilon\,(1-f(\epsilon))\,\rho(\epsilon)\sum_{\mu,\nu}P^{(i)}_{\mu}\times \left|\tilde{V}_{\mu\nu}(x_H,\epsilon)\right|^2\sqrt{\frac{\pi\beta}{\Lambda_{\mu\nu}}}\exp\left[\frac{4\lambda^{(\alpha)}_{\mu\nu}}{\beta\hbar^2\Omega_R^2}\right]\times \exp\left[\frac{-\beta\left(\Delta U_{\mu\nu}+\frac{1}{\beta}\ln\frac{Q^{II}}{Q^I}+\epsilon-e(\eta-\psi)+\Lambda^+_{\mu\nu}\right)^2}{4\Lambda_{\mu\nu}}\right]\times \left\{1-\frac{C^0_{SC^+}}{C^0_{SC}}e^{-\beta e\eta}\right\} \tag{52}$$

In the above expression, the reaction free energy difference, $\Delta G_{\mu\nu}(x_H, \epsilon)$ given in eq 32 has been rewritten using the relation in eq 51 as

$$\Delta G_{\mu\nu}(x_H,\epsilon) = \Delta U_{\mu\nu} + \frac{1}{\beta}\ln\frac{Q^{II}}{Q^I} + \epsilon - e(\eta-\psi) \tag{53}$$

In our definition of the overpotential η, we have defined the reference state to be the equilibrium state with formal electrode potential E^0. In general, the potential ψ at the outer Helmholtz plane also depends on the electrode potential, E.

The anodic and cathodic current densities given in eqs 47 depend on the overpotential, η, through the reaction free energy difference, $\Delta G_{\mu\nu}(x_H, \epsilon)$ given in eq 53. Analysis of the resulting expressions for $j_a(\eta)$ and $j_c(\eta)$, in combination with eq 52 for $j(\eta)$ and the relation $j(\eta) = j_a(\eta) - j_c(\eta)$, leads to the following relation between the anodic and cathodic current densities:

$$j_c(\eta) = j_a(\eta)\frac{C^0_{SC^+}}{C^0_{SC}}e^{-\beta e\eta} \tag{54}$$

Thus, the total nonequilibrium current density can be written in terms of the anodic or cathodic current density as

$$j(\eta) = j_a(\eta)\left\{1-\frac{C^0_{SC^+}}{C^0_{SC}}e^{-\beta e\eta}\right\} = j_c(\eta)\left\{\frac{C^0_{SC}}{C^0_{SC^+}}e^{\beta e\eta}-1\right\} \tag{55}$$

The exchange current density is defined as the anodic or cathodic current density for $\eta = 0$ at equilibrium, where the cathodic and anodic current densities are equal to each other. For electrochemical PCET, this exchange current density, $j_0 = j_a(0) = j_c(0)$, is expressed as

$$j_0 = \frac{F}{\beta'\hbar}C^0_{SC}e^{-z\beta e\psi}\int d\epsilon\,(1-f(\epsilon))\,\rho(\epsilon)\sum_{\mu,\nu}P^{(i)}_{\mu}\times \left|\tilde{V}_{\mu\nu}(x_H,\epsilon)\right|^2\sqrt{\frac{\pi\beta}{\Lambda_{\mu\nu}}}\exp\left[\frac{4\lambda^{(\alpha)}_{\mu\nu}}{\beta\hbar^2\Omega_R^2}\right]\times \exp\left[\frac{-\beta\left(\Delta U_{\mu\nu}+\frac{1}{\beta}\ln\frac{Q^{II}}{Q^I}+\epsilon+e\psi_0+\Lambda^+_{\mu\nu}\right)^2}{4\Lambda_{\mu\nu}}\right] \tag{56}$$

where ψ_0 is the potential at the outer Helmholtz plane when $E = E^0$. The standard heterogeneous rate constant, k_0^{het} is obtained directly from the above expression as

$$k_0^{het} = \frac{j_0}{FC^0_{SC}} \tag{57}$$

In some experimentally studied electrochemical PCET systems, the solute complex is a fixed distance from the metal electrode. For example, the solute complex could be attached to a mixed self-assembled monolayer on the electrode surface.[1−4] For such systems, eq 47 should be replaced by

$$\begin{aligned} j_a &= eC^{cov}_{SC}(r_b)\,k_{SC\to M}(r_b) \\ j_c &= eC^{cov}_{SC^+}(r_b)\,k_{M\to SC^+}(r_b) \end{aligned} \tag{58}$$

where r_b is the distance between the solute complex and the metal electrode, and $C^{cov}_{SC}(r_b)$ and $C^{cov}_{SC^+}(r_b)$ are the coverages for the solute reduced and oxidized forms, respectively, in units of cm^{-2}.[26,76] In this case, the double layer effects are negligible, and all of the equations derived for total current density above will be modified by replacing $FC^0_{SC}\,e^{-z\beta e\psi}/\beta'$ with $eC^{cov}_{SC}(r_b)$ and $FC^0_{SC^+}\,e^{-(z+1)\beta e\psi}/\beta'$ with $eC^{cov}_{SC^+}(r_b)$. The electronic coupling $V^{el}(r_b)$ will depend on the nature of the bridge and can be calculated with previously developed methods for electrochemical electron transfer in such systems.[77−81]

These expressions for rate constants and current densities can be further simplified by making additional approximations. First, we can neglect the effects of the double layer, so $\psi = 0$. Second, we can assume that the density of states $\rho(\epsilon)$ in the electrode is a slowly varying function of energy in the vicinity of the Fermi level and, hence, can be taken out of the integral as a constant $\rho(\mu_M)$. Third, we can assume that the proton transfer is electronically nonadiabatic, so the vibronic couplings factorize into the electronic coupling and the overlap between the corresponding reactant and product proton vibrational wave functions:[71,72]

$$\tilde{V}_{\mu\nu}(x_H,\mu_M) = V^{el}S_{\mu\nu} \tag{59}$$

where V^{el} is the electronic coupling evaluated at x_H and μ_M, and $S_{\mu\nu}$ is the overlap integral evaluated at $\bar{R}_\mu$. Here, we are also invoking the wide band approximation, in which the electronic coupling $V^{el}(x,\epsilon)$ is assumed to be a smooth function of energy, so in the vicinity of the Fermi level of the electrode, it can be approximated as a function of x only: $V^{el}(x, \epsilon) \approx V^{el}(x, \mu_M)$.[82] Fourth, we can assume that the proton potentials are harmonic with frequency ω_H, leading to the following expression for the reaction free energies between pairs of vibronic states given in eq 53 when $\psi = 0$:

$$\Delta G_{\mu\nu}(\epsilon) = \hbar\omega_H(\nu-\mu)+\epsilon-e\eta \tag{60}$$

Note that the ΔU_{00} term no longer appears in the reaction free energies because we utilized the relations $\Delta U_{\mu\nu} = \Delta U_{00} + (\nu - \mu)\hbar\omega_H$ and $1/\beta\,\ln[Q^{II}/Q^I] = -\Delta U_{00}$ that are valid for harmonic proton potentials. In this harmonic approximation, the Boltzmann weights for the reactant and product states simplify to:

$$\begin{aligned} P^{(i)}_{\mu} &= \frac{e^{-\beta\hbar\omega_H(\mu+1/2)}}{e^{\beta\hbar\omega_H/2}-e^{-\beta\hbar\omega_H/2}} \\ P^{(f)}_{\nu} &= \frac{e^{-\beta\hbar\omega_H(\nu+1/2)}}{e^{\beta\hbar\omega_H/2}-e^{-\beta\hbar\omega_H/2}} \end{aligned} \tag{61}$$

The resulting expression for the total current density as a function of the overpotential is

$$j(\eta) = \frac{F}{\beta'\hbar} C^0_{SC}\, \rho(\mu_M) |V^{el}|^2 \int d\epsilon\, (1 - f(\epsilon)) \times \sum_{\mu,\nu} P^{(i)}_{\mu} S^2_{\mu\nu} \sqrt{\frac{\pi\beta}{\Lambda_{\mu\nu}}} \exp\left[\frac{4\lambda^{(\alpha)}_{\mu\nu}}{\beta\hbar^2\Omega_R^2}\right] \times \exp\left[\frac{-\beta(\hbar\omega_H(\nu-\mu) + \epsilon - e\eta + \Lambda^+_{\mu\nu})^2}{4\Lambda_{\mu\nu}}\right] \times \left\{1 - \frac{C^0_{SC^+}}{C^0_{SC}} e^{-\beta e\eta}\right\} \quad (62)$$

and the exchange current density is

$$j_0 = \frac{F}{\beta'\hbar} C^0_{SC} \rho(\mu_M) |V^{el}|^2 \int d\epsilon\, (1 - f(\epsilon)) \times \sum_{\mu,\nu} P^{(i)}_{\mu} S^2_{\mu\nu} \sqrt{\frac{\pi\beta}{\Lambda_{\mu\nu}}} \exp\left[\frac{4\lambda^{(\alpha)}_{\mu\nu}}{\beta\hbar^2\Omega_R^2}\right] \times \exp\left[\frac{-\beta(\hbar\omega_H(\nu-\mu) + \epsilon + \Lambda^+_{\mu\nu})^2}{4\Lambda_{\mu\nu}}\right] \quad (63)$$

As shown in ref 41 for homogeneous PCET, the contributions of the intramolecular solute modes can easily be included in this formulation using methodology developed for electron transfer.[54,55] The resulting electrochemical PCET rate constant expressions for the harmonic treatment of the intramolecular solute modes, as well as the rate constant expressions in the low- and high-temperature limits for these modes, are analogous to those given for homogeneous PCET.[41] In the high-temperature limit for the intramolecular solute modes, the rate constant expressions differ only by a modified reorganization energy, which includes the contribution from the intramolecular (inner-sphere) reorganization. For the expressions given in the present paper, this limit corresponds to adding the inner-sphere reorganization energy, λ_i, to the solvent reorganization energy, λ_s.

D. Comparison to Previous Expressions. The expressions presented in this paper are related to the rate constant expressions for electrochemical PCET utilized by Savéant and co-workers.[5−7,35] However, a number of important differences arise in the present theoretical treatment. An important difference is that the prefactor in their rate expression contains an effective distance that depends on the collision frequency of the solute complex against the electrode surface. This effective distance is determined from the ratio of the prefactor in the adiabatic rate constant expression for heterogeneous ET in an early version of Marcus theory[9] and the standard transition state theory prefactor, k_BT/h. In contrast, we obtain the prefactor in the heterogeneous rate constant expression by explicitly integrating over the distance between the solute complex and the electrode surface,[47] thereby accounting for the effects of extended ET. As shown above, our approach is easily modified for the case of a fixed distance between the solute complex and the electrode. Furthermore, the rate constant expressions given in ref 35 are based on the low-temperature limit for the R mode. As shown in the Appendix, this limit is problematic at high overpotential values. Another difference is that the total reorganization energy in the expressions of Savéant and co-workers is the sum of the solvent and inner sphere reorganization contributions, whereas our total reorganization energy also includes two additional terms, λ_R and $\lambda^{(\alpha)}_{\mu\nu}$, which reflect important aspects of PCET reactions. In particular, $\lambda^{(\alpha)}_{\mu\nu}$, arises from the strong dependence of the vibronic coupling on the proton donor−acceptor distance R. Finally, their expressions are based on the assumption that the reactant and product equilibrium proton donor−acceptor distances are the same (i.e., $\delta R = 0$). In contrast, our expressions include the effects of $\delta R \neq 0$, leading to additional temperature-dependent terms in the effective Marcus theory activation energy. Since these terms differ for the anodic and cathodic current densities, they can result in asymmetries of the Tafel plots, as illustrated below.

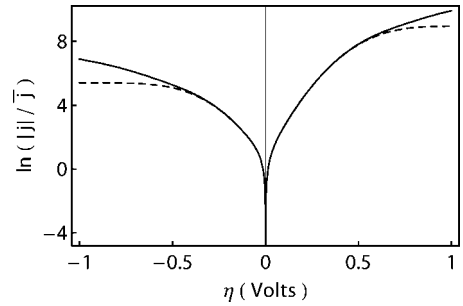

Figure 3. Logarithm of the current density as a function of overpotential at $T = 300$ K for the model system described in the text. The dashed curve is calculated without taking into account the contributions of the excited vibronic states (i.e., including only the ground reactant and product vibronic states). The solid curve represents the fully converged results, which are obtained by including six vibronic states for both the reactant and the product. Here $\bar{j} = \rho(\mu_M) F C^0 |V^{el}|^2/\beta'\hbar$, and the concentrations of the oxidized and reduced species are assumed to be equal (i.e., $C^0_{SC^+} = C^0_{SC} = C^0$).

3. Model Calculations

For the model calculations, we used a simple model with two sets of vibronic states constructed as products of reactant and product electronic states and vibrational states of harmonic oscillators representing the hydrogen atom bonded to its donor and acceptor, respectively. For simplicity, we invoked the set of approximations leading to the current densities in eqs 62 and 63.

For our calculations, we chose parameters that correspond to a physically reasonable electrochemical PCET system. The proton potentials are chosen to be harmonic with frequency $\omega_H = 3000$ cm^{-1}, and the mass of the proton is $m_H = 1$ amu. The equilibrium proton donor−acceptor distance was $\bar{R}_\mu = 2.80$ Å for the reduced solute complex SC and $\bar{R}_\nu = 2.85$ Å for the oxidized solute complex SC$^+$. The donor- and acceptor-hydrogen equilibrium bond lengths were assumed to be 1.0 Å, leading to displacements of the proton oscillators of 0.8 and 0.85 Å, respectively, for the reduced and oxidized forms of the solute complex. The proton donor−acceptor mode R was represented by a harmonic oscillator with frequency $\Omega_R = 100$ cm^{-1} and reduced mass $m_R = 50$ amu. The overlap integrals $S_{\mu\nu}$ at $\bar{R}_\mu$ were calculated analytically for each pair of vibronic states.[83] The parameters $\alpha_{\mu\nu}$ were determined for each pair of vibronic states by calculating the derivatives of the natural logarithm of the corresponding overlap integrals with respect to R at $R = \bar{R}_\mu$. The solvent reorganization energy, λ_s, was chosen to be 10 kcal/mol, which is one-half of a typical value for homogeneous electron transfer in polar solvents. The current densities were calculated by numerical integration of eq 62.

The calculated Tafel plots are shown in Figures 3 and 4. As in the case of electron transfer, the current density reaches a plateau value at high negative and positive overpotentials. In these regions, the contributions of the excited vibronic states of the solute complex become extremely important, as illustrated in Figure 3. To achieve convergence in the calculations for high absolute values of the overpotential ($|\eta| > 0.5$ V), we had to

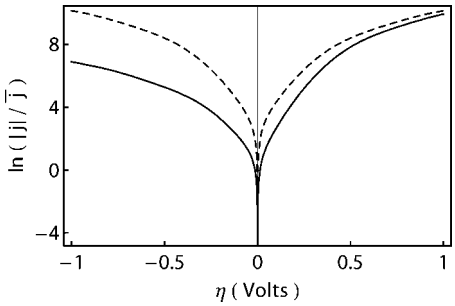

Figure 4. Logarithm of the current density as a function of overpotential at $T = 300$ K for the model system described in the text. The solid and dashed curves correspond to $\delta R = 0.05$ Å and $\delta R = 0$, respectively. For both curves, six vibronic states are included for both the reactant and the product. Here $\bar{j} = \rho(\mu_M)FC^0|V^{el}|^2/\beta'\hbar$, and the concentrations of the oxidized and reduced species are assumed to be equal (i.e., $C^0_{SC^+} = C^0_{SC} = C^0$).

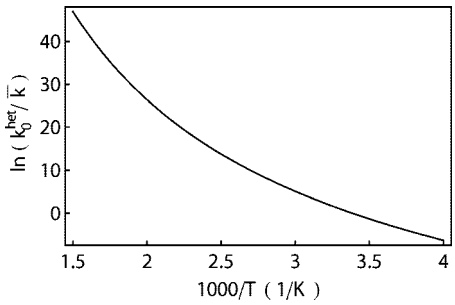

Figure 5. An Arrhenius plot of the standard oxidation rate constant k_0^{het}. Here $\bar{k} = \rho(\mu_m)|V^{el}|^2/\beta'\hbar$.

include at least six proton vibrational states for the reactant and product states. At small overpotentials, we observed the linear Butler−Volmer regions used to extract the transfer coefficients for the cathodic and anodic processes.[74] In the case of electrochemical electron transfer with large solvent reorganization energy, the transfer coefficient, α, at small overpotentials is close to 1/2, and the Tafel plot is symmetric with respect to $\eta = 0$. In the case of electrochemical PCET, we observe noticeably asymmetric Tafel plots when the equilibrium proton donor−acceptor distances for the reduced and oxidized solute complexes differ (i.e., $\delta R \neq 0$).

The transfer coefficients at small η are still close to 1/2, but a significant deviation is observed at larger η values. We can estimate the cathodic transfer coefficient α_{PCET} at small η by neglecting the contributions of the excited states and assuming that the electron is transferred from the Fermi level of the electrode. In this case,

$$\alpha_{PCET}(\eta) \approx \frac{1}{2} - \frac{\alpha_{00}\,\delta R}{\beta\Lambda_{00}} + \frac{e\eta}{2\Lambda_{00}} \tag{64}$$

Note that the second term in the above expression is proportional to the absolute temperature, so the asymmetry will increase with temperature.

The temperature dependence of the standard oxidation rate constant at $\eta = 0$ is shown in Figure 5. This figure illustrates the same features as observed in the cases of homogeneous nonadiabatic PCET and homogeneous nonadiabatic PT reactions. Specifically, we observe pronounced non-Arrhenius behavior at high temperatures, leading to enhancement of the rate, and linear Arrhenius behavior at lower temperatures.

4. Summary and Concluding Remarks

In this paper, we have derived expressions for the nonadiabatic transition probabilities, the heterogeneous rate constants, and the current densities of electrochemical PCET reactions. Our systematic derivations provide expressions based on a series of well-defined approximations. Equation 26 is an expression for the probability flux correlation function that can be used in conjunction with eq 17 to calculate transition probabilities, which in turn can be used to calculate rate constants and current densities. The advantage of eq 26 is that it is expressed in terms of time correlation functions of the energy gap and the R mode, without any harmonic approximations for the solvent or the R mode. These correlation functions can be determined from classical molecular dynamics trajectories for the system moving on the reactant vibronic energy surface. Invoking the harmonic approximation for the solvent modes and the R mode leads to eqs 29 and 37 for the transition probabilities corresponding to oxidation and reduction, respectively. Closed analytical expressions can be obtained in the high-temperature limit for the R mode and the solvent modes, leading to eqs 35 and 39 for the transition probabilities corresponding to oxidation and reduction, respectively. In all cases, these transition probabilities can be converted to rate constants through eqs 42 and to current densities through eqs 43. The analytical expressions for rate constants and current densities can be further simplified by assuming that the rate constants decrease exponentially with the distance x between the solute complex and the electrode surface and that the concentrations of oxidized and reduced species depend on x according to eqs 45. These approximations lead to the expression in eq 52 for total current density as a function of the overpotential η. The total current density can be converted to anodic and cathodic current densities as functions of the overpotential through eq 55. If several additional, well-defined approximations are made, the simplified expressions in eqs 62 and 63 for total current density and exchange current density are obtained.

The expressions presented in this paper are similar to the expressions describing nonadiabatic electrochemical electron transfer.[9,12,57] However, a number of important differences arise for electrochemical PCET processes. The electrochemical PCET rate constants are calculated by summing over the reactant and product electron−proton vibronic states. The excited vibronic states become particularly important at high voltages. Although solute modes can be included in electrochemical electron transfer, typically these solute modes are assumed to be harmonic and uncoupled to the solvent, leading to a separation between the electronic coupling and the Franck−Condon overlap of the solute modes. In contrast, for PCET reactions, the transferring proton is strongly coupled to the solvent, and the proton potential for each electron transfer state is typically asymmetric with significant anharmonic effects for the excited states. In general, the nonadiabatic coupling between reactant and product mixed electron−proton vibronic states for PCET reactions cannot be expressed as the product of the electronic coupling and the overlap between the proton vibrational wave functions. However, this separation is valid in the limit of electronically nonadiabatic proton transfer.[71,72] As in electrochemical electron transfer, the electronic coupling depends exponentially on the distance between the solute complex and the electrode surface. An important difference is that the vibronic coupling for PCET reactions also depends strongly on the proton donor−acceptor distance.

The modulation of the vibronic coupling by the proton donor−acceptor vibrational motion leads to three significant differences in the electrochemical PCET rate constant expressions. First, the total reorganization energy includes two additional contributions: the reorganization energy of the proton

donor−acceptor mode and a coupling term associated with the modulation of the vibronic coupling by this mode. Second, the rate constants include an additional exponential temperature-dependent prefactor that depends on the frequency of the proton donor−acceptor mode and the α parameter characterizing the modulation of the vibronic coupling by this mode. As in the case of homogeneous nonadiabatic PCET[42] and homogeneous nonadiabatic PT,[51,53] this additional prefactor leads to non-Arrhenius behavior of the rate constant at higher temperatures. Third, the effective Marcus theory activation energies contain temperature-dependent terms arising from the change in the equilibrium proton donor−acceptor distance upon electron transfer. This term has a different sign for the cathodic and anodic processes, leading to asymmetries of the theoretical Tafel plots, even for small changes in the equilibrium proton donor−acceptor distance. It also leads to an additional temperature-dependent term in the cathodic transfer coefficient.

The application of the theory presented in this paper to experimentally studied systems will enable us to test the various approximations and determine the level of theory required for a specified level of accuracy. On the basis of previous calculations of homogeneous PCET reactions,[60,84] we expect that the analytical expressions will be capable of reproducing qualitative trends and will assist in interpreting experimental data. A significant prediction generated by this theory is that the Tafel plots will become more asymmetric as the difference between the equilibrium proton donor−acceptor distances for the oxidized and reduced states of the solute complex increases. This prediction provides an experimental diagnostic for electrochemical PCET. The application of this theory to specific electrochemical PCET systems should provide additional insight into the underlying physical principles and lead to experimentally testable predictions.

Appendix

Low Temperature Limit of the Rate Constant

The rate constants for oxidation and reduction can also be evaluated at the low temperature limit for the *R* mode ($\beta\hbar\Omega_R \gg 1$) and the high temperature limit for the solvent modes ($\beta\hbar\omega_c \ll 1$). In this case, the transition probability of PCET from the reduced solute complex (SC) located at a distance x_H from the electrode surface to a one-electron state in the electrode with energy ϵ_m is

$$W_{SC\rightarrow M}(x_H,\epsilon_m) = \frac{1}{\hbar^2}\sum_{\mu,\nu} P_\mu^{(i)}\left|\tilde{V}_{\mu\nu}(x_H,\epsilon_m)\right|^2 \exp\left[\frac{\lambda_{\mu\nu}^{(\alpha)}-\lambda_R}{\hbar\Omega_R}-\alpha_{\mu\nu}\delta R\right]\times \int_{-\infty}^{\infty} dt \exp\left[\frac{it}{\hbar}(\Delta G_{\mu\nu}(x_H,\epsilon_m)+\lambda_s)+\left(\frac{\lambda_{\mu\nu}^{(\alpha)}+\lambda_R}{\hbar\Omega_R}+\alpha_{\mu\nu}\delta R\right)e^{i\Omega_R t}-\frac{\lambda_s t^2}{\hbar^2\beta}\right] \quad (A.1)$$

with the free energy difference $\Delta G_{\mu\nu}(x_H,\epsilon_m)$ given in eq 53. Following the work of Borgis and Hynes for nonadiabatic PT,[52] the time integral can be evaluated using the stationary phase approximation. Under the condition $\lambda_s > |\Delta G_{\mu\nu}(x_H,\epsilon_m)|$, the following Marcus-like expression is obtained:

$$W_{SC\rightarrow M}(x_H,\epsilon_m) = \frac{1}{\hbar}\sum_{\mu,\nu} P_\mu^{(i)}\left|\tilde{V}_{\mu\nu}(x_H,\epsilon_m)\right|^2 \sqrt{\frac{\pi\beta}{\lambda_s}}\times \exp\left[\frac{\lambda_{\mu\nu}^{(\alpha)}-\lambda_R}{\hbar\Omega_R}-\alpha_{\mu\nu}\delta R\right]\exp\left[\frac{-\beta(\Delta G_{\mu\nu}(x_H,\epsilon_m)+\lambda_s)^2}{4\lambda_s}\right] \quad (A.2)$$

Note that the free energy difference $\Delta G_{\mu\nu}(x_H,\epsilon_m)$ is a function of the overpotential η of the electrode, as well as the energy ϵ_m of the metal electron state and the distance x_H between the solute complex and the electrode surface. As a result, the low temperature limit expression given in eq A.2 can be used only when the overpotential η and the energy ϵ_m are sufficiently low to maintain the inequality $\lambda_s > |\Delta G_{\mu\nu}(x_H,\epsilon_m)|$.

The transition probability for reduction of the solute complex SC^+ in the low temperature limit for the *R* mode and the high temperature limit for the solvent modes is

$$W_{M\rightarrow SC^+}(x_H,\epsilon_m) = \frac{1}{\hbar^2}\sum_{\mu,\nu} P_\nu^{(f)}\left|\tilde{V}_{\mu\nu}(x_H,\epsilon_m)\right|^2 \exp\left[\frac{\lambda_{\mu\nu}^{(\alpha)}-\lambda_R}{\hbar\Omega_R}-\alpha_{\mu\nu}\delta R\right]\times \int_{-\infty}^{\infty} dt \exp\left[\frac{it}{\hbar}(-\Delta G_{\mu\nu}(x_H,\epsilon_m)+\lambda_s)+\left(\frac{\lambda_{\mu\nu}^{(\alpha)}+\lambda_R}{\hbar\Omega_R}-\alpha_{\mu\nu}\delta R\right)e^{i\Omega_R t}-\frac{\lambda_s t^2}{\hbar^2\beta}\right] \quad (A.3)$$

The analytical expression obtained using the stationary phase approximation under the condition $\lambda_s > |\Delta G_{\mu\nu}(x_H,\epsilon_m)|$ is

$$W_{M\rightarrow SC^+}(x_H,\epsilon_m) = \frac{1}{\hbar}\sum_{\mu,\nu} P_\nu^{(f)}\left|\tilde{V}_{\mu\nu}(x_H,\epsilon_m)\right|^2 \sqrt{\frac{\pi\beta}{\lambda_s}}\times \exp\left[\frac{\lambda_{\mu\nu}^{(\alpha)}-\lambda_R}{\hbar\Omega_R}-\alpha_{\mu\nu}\delta R\right]\exp\left[\frac{-\beta(\Delta G_{\mu\nu}(x_H,\epsilon_m)+\lambda_s)^2}{4\lambda_s}\right] \quad (A.4)$$

In contrast to the high temperature limit, the reorganization energy, λ_s, in the effective activation energy and the pre-exponential term are the same for both oxidation and reduction transition probabilities. The standard heterogeneous rate constants and the current densities can also be evaluated in this limit using the same procedures as described above.

Acknowledgment. We are grateful to Irina Navrotskaya for helpful discussions. This work was supported by NSF Grant No. CHE-05-01260.

References and Notes

(1) Finklea, H. O; Haddox, R *Phys. Chem. Chem. Phys.* **2001**, *3*, 3431–3436.
(2) Haddox, R.; Finklea, H. O. *J. Electroanal. Chem.* **2003**, *550−551*, 351–358.
(3) Haddox, R.; Finklea, H. O. *J. Phys. Chem. B* **2004**, *108*, 1694–1700.
(4) Madhiri, N.; Finklea, H. O. *Langmuir* **2006**, *22*, 10643–51.
(5) Costentin, C.; Evans, D. H.; Robert, M.; Savéant, J.-M.; Singh, P. S. *J. Am. Chem. Soc.* **2005**, *127*, 12490–12491.
(6) Costentin, C.; Robert, M.; Savéant, J.-M. *J. Am. Chem. Soc.* **2006**, *128*, 8726–8727.
(7) Costentin, C.; Robert, M.; Savéant, J.-M. *J. Am. Chem. Soc.* **2007**, *129*, 9953–9963.
(8) Costentin, C.; Robert, M.; Savéant, J.-M. *J. Am. Chem. Soc.* **2006**, *128*, 4552–4553.
(9) Marcus, R. A. *Annu. Rev. Phys. Chem.* **1964**, *15*, 155–196.

(10) Marcus, R. A.; Sutin, N. *Biochim. Biophys. Acta* **1985**, *811*, 265–322.
(11) Newton, M. D.; Sutin, N. *Annu. Rev. Phys. Chem.* **1984**, *35*, 437–480.
(12) Levich, V. G. In *Physical Chemistry: an Advanced Treatise*; Eyring, H., Henderson, D., Jost, W., Eds.; Academic Press: New York, London, 1970; Vol. IXB, pp 985−1074..
(13) Hush, N. S. *J. Electroanal. Chem.* **1999**, *460*, 5–29.
(14) Dogonadze, R. R. In *Reactions of Molecules at Electrodes*; Hush, N. S., Ed.; Wiley-Interscience: New York, 1971, Chapter *3*, pp 135−227.
(15) Gorodyski, A. V.; Dvali, V. G.; Dogonadze, R. R.; Marsagishvili, T. A. *Ukr. Khim. Zh.* **1983**, *49*, 836–838.
(16) Dogonadze, R. R.; Chonishvili, G. M.; Marsagishvili, T. A. *J. Chem. Soc., Faraday Trans.* **1984**, *80*, 355–364.
(17) Gorodyskii, A.; Karasevskii, A.; Matyushov, D. V. *J. Electroanal. Chem. Interfacial Chem.* **1991**, *315*, 9–28.
(18) Chandler, D. In *Computer Simulation of Rare Events and Dynamics of Classical and Quantum Condensed-Phase Systems−Classical and Quantum Dynamics in Condensed Phase Simulations*; Berne, B. J., Ciccotti, G., Coker, D. F., Eds.; World Science: Singapore, 1998, pp 25−49..
(19) Sebastian, K. L.; Tachiya, M. *J. Chem. Phys.* **2006**, *124*, 064713.
(20) Sebastian, K. L. *J. Chem. Phys.* **1989**, *90*, 5056–5067.
(21) Matyushov, D. V. *J. Electroanal. Chem.* **1994**, *367*, 1–6.
(22) Matyushov, D. V. *Chem. Phys.* **1992**, *164*, 31–46.
(23) Boroda, Y. G.; Voth, G. A. *J. Chem. Phys.* **1996**, *104*, 6168–6183.
(24) Calhoun, A.; Voth, G. A. *J. Phys. Chem.* **1996**, *100*, 10746–10753.
(25) Schmickler, W. *Electrochim. Acta* **1996**, *41*, 2329–2338.
(26) Royea, W. J.; Fajardo, A. M.; Lewis, N. S. *J. Phys. Chem. B* **1997**, *101*, 11152–11159.
(27) Boroda, Y. G.; Calhoun, A.; Voth, G. A. *J. Chem. Phys.* **1997**, *107*, 8940–8954.
(28) Schmickler, W.; Mohr, J. *J. Chem. Phys.* **2002**, *117*, 2867–2872.
(29) Benderskii, V. A.; Grebenshchikov, S. Y. *J. Electroanal. Chem.* **1994**, *375*, 29–44.
(30) Calhoun, A.; Koper, M. T. M.; Voth, G. A. *J. Phys. Chem. B* **1999**, *103*, 3442–3448.
(31) Schmickler, W. *Chem. Phys. Lett.* **2000**, *317*, 458–463.
(32) Ignaczak, A.; Schmickler, W. *J. Electroanal. Chem.* **2003**, *554−555*, 201–209.
(33) Santos, E.; Koper, M.; Schmickler, W. *Chem. Phys. Lett.* **2006**, *419*, 421–425.
(34) Grimminger, J.; Bartenschlager, S.; Schmickler, W. *Chem. Phys. Lett.* **2005**, *416*, 316–320.
(35) Costentin, C.; Robert, M.; Savéant, J.-M. *J. Electroanal. Chem.* **2006**, *588*, 197–206.
(36) Grimminger, J.; Schmickler, W. *Chem. Phys.* **2007**, *334*, 8–17.
(37) Warshel, A. In *Computer Modeling of Chemical Reactions in Enzymes and Solutions*; Wiley: New York, 1991.
(38) Cukier, R. I. *J. Phys. Chem.* **1996**, *100*, 15428–15443.
(39) Cukier, R. I.; Nocera, D. G. *Annu. Rev. Phys. Chem.* **1998**, *49*, 337–369.
(40) Soudackov, A. V.; Hammes-Schiffer, S. *J. Chem. Phys.* **1999**, *111*, 4672–4687.
(41) Soudackov, A.; Hammes-Schiffer, S. *J. Chem. Phys.* **2000**, *113*, 2385–2396.
(42) Soudackov, A.; Hatcher, E.; Hammes-Schiffer, S. *J. Chem. Phys.* **2005**, *122*, 014505.
(43) Costentin, C.; Robert, M.; Savéant, J.-M. *J. Am. Chem. Soc.* **2007**, *129*, 5870–5879.
(44) Anderson, P. W. *Phys. Rev.* **1961**, *124*, 41–53.
(45) Newns, D. M. *Phys. Rev.* **1969**, *178*, 1123–1135.
(46) Navrotskaya, I.; Soudackov, A. V.; Hammes-Schiffer, S. *J. Chem. Phys.* **2008,** *128*, 244712.
(47) Gavaghan, D. J.; Feldberg, S. W. *J. Electroanal. Chem.* **2000**, *491*, 103–110.
(48) Trakhtenberg, L. I.; Klochikhin, V. L.; Pshezhetsky, S. Y. *Chem. Phys.* **1981**, *59*, 191–198.
(49) Trakhtenberg, L. I.; Klochikhin, V. L.; Pshezhetsky, S. Y. *Chem. Phys.* **1982**, *69*, 121–134.
(50) Borgis, D.; Lee, S. Y.; Hynes, J. T. *Chem. Phys. Lett.* **1989**, *162*, 19–26.
(51) Borgis, D.; Hynes, J. T. *J. Chem. Phys.* **1991**, *94*, 3619–3628.
(52) Borgis, D.; Hynes, J. T. *Chem. Phys.* **1993**, *170*, 315–346.
(53) Suarez, A.; Silbey, R. *J. Chem. Phys.* **1991**, *94*, 4809–4816.
(54) Kestner, N. R.; Logan, J.; Jortner, J. *J. Phys. Chem.* **1974**, *78*, 2148–2166.
(55) Ulstrup, J.; Jortner, J. *J. Chem. Phys.* **1975**, *63*, 4358–4368.
(56) Kim, H. J.; Hynes, J. T. *J. Chem. Phys.* **1992**, *96*, 5088–5110.
(57) Marcus, R. A. *J. Chem. Soc., Faraday Trans.* **1996**, *92*, 3905–3908.
(58) Soudackov, A.; Hammes-Schiffer, S. *Chem. Phys. Lett.* **1999**, *299*, 503–510.
(59) Kubo, R. *J. Phys. Soc. Jpn.* **1962**, *17*, 1100.
(60) Hatcher, E.; Soudackov, A.; Hammes-Schiffer, S. *J. Phys. Chem. B* **2005**, *109*, 18565–18574.
(61) Hatcher, E.; Soudackov, A. V.; Hammes-Schiffer, S. *J. Am. Chem. Soc.* **2007**, *129*, 187–196.
(62) Calhoun, A.; Voth, G. A. *J. Chem. Phys.* **1998**, *109*, 4569–4575.
(63) Calhoun, A.; Voth, G. A. *J. Electroanal. Chem.* **1998**, *450*, 253–264.
(64) Calhoun, A.; Koper, M. T. M.; Voth, G. A. *Chem. Phys. Lett.* **1999**, *305*, 94–100.
(65) Guidelli, R.; Schmickler, W. *Electrochim. Acta* **2000**, *45*, 2317–2338.
(66) Kuznetsov, A.; Schmickler, W. *Chem. Phys. Lett.* **2000**, *327*, 314–318.
(67) Ignaczak, A.; Schmickler, W. *Chem. Phys.* **2002**, *278*, 147–158.
(68) Levich, V. G. In *Advances in Electrochemistry and Electrochemical Engineering*; Delahey, P., Ed.; Interscience: New York, 1966, Vol. 4, pp 249−372.
(69) Mukamel, S. *Principles of Nonlinear Optical Spectroscopy*; Oxford University Press: New York, 1995.
(70) Ohta, Y.; Soudackov, A. V.; Hammes-Schiffer, S. *J. Chem. Phys.* **2006**, *125*, 144522.
(71) Georgievskii, Y.; Stuchebrukhov, A. A. *J. Chem. Phys.* **2000**, *113*, 10438–10450.
(72) Skone, J.; Soudackov, A.; Hammes-Schiffer, S. *J. Am. Chem. Soc.* **2006**, *128*, 16655–16663.
(73) Feldberg, S.; Sutin, N. *Chem. Phys.* **2006**, *324*, 216–225.
(74) Bard, A. J.; Faulkner, L. R. *Electrochemical Methods: Fundamentals and Applications*; Wiley: New York, 1980.
(75) Shaw, D. J. *Introduction to Colloid and Surface Chemistry*; Butterworth-Heinemann: Boston, 1992.
(76) Traub, M. C.; Brunschwig, B. S.; Lewis, N. S. *J. Phys. Chem. B* **2007**, *111*, 6676–6683.
(77) Gosavi, S.; Gao, Y. Q.; Marcus, R. A. *J. Electroanal. Chem.* **2001**, *500*, 71–77.
(78) Gosavi, S.; Marcus, R. A. *J. Phys. Chem. B* **2000**, *104*, 2067–2072.
(79) Hsu, C. P.; Marcus, R. A. *J. Chem. Phys.* **1997**, *106*, 584–598.
(80) Newton, M. D.; Smalley, J. F. *Phys. Chem. Chem. Phys.* **2007**, *9*, 555–572.
(81) Smalley, J. F.; Newton, M. D.; Feldberg, S. W. *J. Electroanal. Chem.* **2006**, *589*, 1–6.
(82) Chidsey, C. E. D. *Science* **1991**, *251*, 919–922.
(83) Chang, J. L. *J. Mol. Spectrosc.* **2005**, *232*, 102–104.
(84) Hammes-Schiffer, S.; Iordanova, N. *Biochim. Biophys. Acta* **2004**, *1655*, 29–36.

JP802171Y